Optimized chemistry for Large Eddy Simulations of wrinkled flames

Cédric Mehl, Mélodie Cailler, Renaud Mercier, Vincent Moureau, Benoit Fiorina

Proceedings of the Combustion Institute

Optimized chemistry for Large Eddy Simulations of wrinkled flames

--Manuscript Draft--

Manuscript Number:	
Article Type:	5. Turbulent Flames
Keywords:	Turbulent combustion modelling; Large Eddy Simulation; pollutants; flame wrinkling
Corresponding Author:	Cédric Mehl IFP Energies nouvelles Rueil Malmaison, FRANCE
First Author:	Cédric Mehl
Order of Authors:	Cédric Mehl
	Mélody Cailler
	Renaud Mercier
	Vincent Moureau
	Benoit Fiorina
Abstract:	State-of-the-art LES models have made significant progress in the prediction of heat release and flame propagation for a wide range of combustion regimes. Predicting pollutants remains however a difficult issue, especially in situations where sub-grid scale wrinkling is high. A novel strategy, named COPLES (Chemistry OPtimized for LES), is presented in this paper to account for the effect of sub-grid scale wrinkling on pollutants formation in a transported chemistry context and under flamelet regime assumption. New chemical mechanisms are built through an optimization process to recover the properties of filtered flames. Two alternative formulations are proposed. The first one consists in optimizing the COPLES parameters to retrieve the structure of Filtered Planar Flame (FPF) and to include separately the impact of sub-grid scale wrinkling. The second formulation targets directly a collection of Filtered Wrinkled Flamelets (FWF), so that the influence of turbulence on the chemical flame structure is intrinsically accounted for. The two approaches are successfully validated on 1-D freely propagating premixed flames and then challenged against the standard Thickened Flame for LES model on a turbulent premixed swirled combustor, experimented at Cambridge University. Whereas all formulations retrieve the temperature field, the COPLES-FWF model improves significantly the prediction of CO formation.

38^{th} International Symposium on Combustion

Optimized chemistry for Large Eddy Simulations of wrinkled flames

C. Mehl[1] , M. Cailler[1], R. Mercier[2], V. Moureau[3], B. Fiorina[1]

[1] Laboratoire EM2C, CNRS, CentraleSupélec, Université Paris-Saclay, 3 rue Joliot Curie, 91190 Gif-sur-Yvette, France

[2] Safran tech, Modelling & Simulation, Rue des Jeunes Bois, Châteaufort, 78114 Magny-les-Hameaux, France

[3] CORIA- CNRS UMR 6614-Normandie Université - Université et INSA de Rouen, Campus Universitaire du Madrillet, 76800 Saint Etienne du Rouvray, Rouen, France

Colloquium: TURBULENT FLAMES.

Corresponding author: Cédric Mehl

- address: 1-4 avenue de Bois-Préau, 92852 Rueil-Malmaison Cedex, France
- e-mail: cedric.mehl@ifpen.fr

WORD COUNT

Method of determination: Method 2

Words in text: 3215

Words in references: 540

Words in tables: 54

Words in equations: 276

Words in figures: 1715

Total length of paper: 5800 words

I agree to pay color reproduction charges if applicable

Optimized chemistry for Large Eddy Simulations of wrinkled flames

C. Mehl[a,*], M. Cailler[a,b], R. Mercier[b], V. Moureau[c], B. Fiorina[a]

[a] *Laboratoire EM2C, CNRS, CentraleSupélec, Université Paris-Saclay, 3 rue Joliot Curie, 91190 Gif-sur-Yvette, France*
[b] *SAFRAN Tech, Rue des Jeunes Bois, Châteaufort - CS 80112, 78772 Magny-les-Hameaux, France*
[c] *CORIA- CNRS UMR 6614-Normandie Université - Université et INSA de Rouen, Campus Universitaire du Madrillet, 76800 Saint Etienne du Rouvray, Rouen, France*

Abstract

State-of-the-art LES models have made significant progress in the prediction of heat release and flame propagation for a wide range of combustion regimes. Predicting pollutants remains however a difficult issue, especially in situations where sub-grid scale wrinkling is high. A novel strategy, named COPLES (Chemistry OPtimized for LES), is presented in this paper to account for the effect of sub-grid scale wrinkling on pollutants formation in a transported chemistry context and under flamelet regime assumption. New chemical mechanisms are built through an optimization process to recover the properties of filtered flames. Two alternative formulations are proposed. The first one consists in optimizing the COPLES parameters to retrieve the structure of Filtered Planar Flame (FPF) and to include separately the impact of sub-grid scale wrinkling. The second formulation targets directly a collection of Filtered Wrinkled Flamelets (FWF), so that the influence

*Corresponding author
Email address: cedric.mehl@centralesupelec.fr (C. Mehl)

of turbulence on the chemical flame structure is intrinsically accounted for. The two approaches are successfully validated on 1-D freely propagating premixed flames and then challenged against the standard Thickened Flame for LES model on a turbulent premixed swirled combustor, experimented at Cambridge University. Whereas all formulations retrieve the temperature field, the COPLES-FWF model improves significantly the prediction of CO formation.

Keywords: Turbulent combustion modeling, Large Eddy Simulation, pollutants, flame wrinkling

2010 MSC: 00-01, 99-00

---

1. Introduction

Prediction of pollutants formation in Large Eddy Simulation (LES) requires complex chemistry [1]. Issues relative to the computational cost induced by detailed chemistry are tackled by resorting either to chemistry reduction [2] or to tabulation techniques [3, 4]. By storing in a pre-processing step all thermo-chemical information in a look-up table, tabulated chemistry is extremely competitive in terms of CPU time. However, it lacks flexibility when the encountered flame structures differ from the tabulated archetypes [5]. Large discrepencies on the prediction of CO in a diluted combustion burner were for instance observed in the work of Lamouroux *et al.* [6]. Meanwhile, the progress in reduced mechanisms and the increase of available computational power enable a direct use of transported chemistry. Recently, analytic mechanisms have been for example introduced in LES [7, 8]. Also, virtual optimized schemes, developed to capture both heat release [9] and pollutant formation [10, 11] over a wide range of flame regimes have been successfully applied to LES of turbulent premixed flames.

Within both reduced and tabulated chemistry formalisms, the closure of filtered species balance equations is the key of turbulent combustion modeling. The LES combustion model must address two issues [12]: (i) it has to handle situations where the flame front is thinner than the LES grid. Commonly used solutions are either to filter [13] or thicken [14] the species equations at a scale larger than the mesh size; (ii) it must include a model for integrating sub-grid scale turbulent effects, for instance through a wrinkling factor [15] or a FDF [16]. We focus here on models based on a geometrical description of the flame front [12], which are efficient to compute flames in

complex geometries at low computational costs. While geometrical models have been able to predict heat release and flame propagation in various conditions [7, 13], intermediate species prediction remains challenging [17]. A recent work by Abou-Taouk *et al.* [18] has focused on the inclusion of (i) directly in the reaction mechanism by optimizing Arrhenius parameters on filtered flames. The method recovers well the structure of filtered planar laminar flames but is not able to predict intermediate species concentrations if the flame is wrinkled.

Indeed, as observed in a turbulent flame DNS [19], filtered quantities, especially intermediate species such as CO, are influenced by the surface of the flame contained at the sub-filter scale. The recent work developed by Mercier *et al.* [20] includes these effects on pollutant formation by defining a new flame archetype, which takes sub-grid scale flame wrinkling intrinsically into account. The model relies on the Filtered Wrinkled Flamelets (FWF) archetype, obtained by manufacturing two-dimensional wrinkled flames, which are filtered at the LES filter size. FWF has been used to build-up a filtered chemical look-up table in order to model the unclosed terms of the filtered progress variable equation. Simulations of the swirling stabilized Cambridge flame [21] showed that accounting for sub-filter flame wrinkling on the chemical flame structure improves the prediction of intermediate species such as CO [20]. Whereas the benefit of FWF has been demonstrated within a tabulated chemistry framework, accounting for the impact of SGS flame wrinkling on the species formation in a reduced chemistry context remains an open question.

The objective of the present work is to extend the work of Mercier *et*

al. [20] in a reduced chemistry context. Developments are made under a flamelet regime assumption. Contrarily to classical LES models [14], the impact of sub-filter turbulence on CO formation [22, 20] is accounted for. Other physical phenomena which may impact the formation of CO, such as flame generated turbulence or counter-gradient transport, are not tackled. The selected methodology features the development of optimized filtered schemes to retrieve the properties of the FWF flame archetype. The paper is organized as follow: model equations are detailed in Sec. 2, the filtered mechanism generation is presented in Sec. 3 whereas validations in both 1-D and 3-D turbulent premixed flames configurations are shown in Sec. 4.

2. Chemistry Optimized for LES of turbulent flames

2.1. Model equations

In LES, the balance equation of the filtered species mass fraction $\widetilde{Y}_k$ reads:

$$\frac{\partial \overline{\rho}\widetilde{Y}_k}{\partial t} + \nabla \cdot \left(\overline{\rho}\widetilde{u}\widetilde{Y}_k\right) = \overline{\mathrm{RHS}(\mathbf{\Phi})} \tag{1}$$

where u is the flow velocity and $\mathbf{\Phi} = (P, T, Y_1, ..., Y_N)$ is the thermo-chemical state vector with P and T the pressure and temperature. $\overline{\varphi}$ and $\widetilde{\varphi}$ denote Reynolds and Favre averaging of quantity φ, respectively. The unclosed filtered Right Hand Side $\overline{\mathrm{RHS}(\mathbf{\Phi})}$ reads:

$$\overline{\mathrm{RHS}(\mathbf{\Phi})} = \overline{\tau}_k + \nabla \cdot \left(\overline{\rho D_k \nabla Y_k}\right) + \overline{\rho \dot{\omega}_k^{\mathcal{A}}(\mathbf{\Phi})} \tag{2}$$

where D_k is the molecular diffusivity of species k, $\overline{\tau}_k = -\nabla \cdot (\widetilde{\overline{\rho}u\overline{Y_k}} - \overline{\rho}\widetilde{u}\widetilde{Y}_k)$ is the sub-grid scale convective term and $\dot{\omega}_k$ the chemical reaction rate of

species k parametrized by the set of kinetic rate parameters $\mathcal{A}$. Because of non-linearities of the terms that compose Eq.2, the RHS cannot be directly estimated from the filtered thermochemical variable [12]: $\overline{\mathrm{RHS}(\mathbf{\Phi})} \neq \mathrm{RHS}(\overline{\mathbf{\Phi}})$.

The concept of Chemistry OPtimized for LES (COPLES) is to identify a function RHS*, which verifies the equality $\overline{\mathrm{RHS}(\mathbf{\Phi})} = \mathrm{RHS}^*(\overline{\mathbf{\Phi}})$. The following formulation of RHS* is retained for that purpose:

$$\mathrm{RHS}^* = \nabla \cdot \left(\overline{\rho} \alpha^* \widetilde{D} \nabla \widetilde{Y}_k \right) + \overline{\rho} \widetilde{\dot{\omega}}_k^{\mathcal{A}^*} \tag{3}$$

with:

$$\overline{\rho} \widetilde{\dot{\omega}}_k^{\mathcal{A}^*} = W_i \sum_{j=1}^{N_R} A_j^* \left(\nu_{kj}^b - \nu_{kj}^f \right) \times \prod_{i \in \mathcal{S}_j} \left(\frac{\overline{\rho} \widetilde{Y}_i}{W_i} \right)^{n_{ij}^*} \exp\left(\frac{-E_{a,j}^*}{\mathcal{R} \widetilde{T}} \right) \tag{4}$$

where N_R is the number of reactions, $\mathcal{S}_j$ are the species involved in reaction j, and ν_{kj}^b, ν_{kj}^f are respectively the backward and forward stoechiometric coefficients of species k in reaction j. Variables with * superscripts are model parameters: α^* is constant in space and identical for each species and $\mathcal{A}^* = (A_j^*, E_{a,j}^*, n_{ij}^*)$ where A_j^* are the pre-exponential constants, $E_{a,j}^*$ the activation energies and n_{ij}^* the reaction orders of the modeled chemical mechanism.

The parameters are optimized through a genetic algorithm [9, 11] to recover the properties of an ensemble made of N canonical 1-D target flames. The optimization process consists in minimizing the following function:

$$\zeta(\mathcal{A}^*, \alpha^*) = \sum_{n=1}^{N} \left(\frac{\| \widetilde{\varphi}_n^* - \widetilde{\varphi}_n^{ref} \|_2}{\| \widetilde{\varphi}_n^{ref} \|_2} + \beta \frac{\mid f_{\varphi,n}^* - f_{\varphi,n}^{ref} \mid}{f_{\varphi,n}^{ref}} \right) \tag{5}$$

where φ_n and $f_{\varphi,n}$ are respectively the thermo-chemical spatial profile and the specific global flame properties of the n-th 1-D flame targeted by the

optimized scheme. Superscript *ref* and $*$ refer to the target flame and to the solution obtained with optimized parameters, respectively. β is a weighting parameter set to 1 in the present work.

The choice of the reference canonical flames is critical. The retained filtered archetype must be representative of the sub-grid turbulent flame structure encountered for various level of sub-grid flame wrinkling. As discussed in [20], the issue is to account for the influence of the subfilter flame front geometry on the pollutant formation at the resolved scale. Two archetypes are discussed in the following section: the Filtered Planar Flames (FPF) and the Filtered Wrinkled Flamelets (FWF).

2.2. Reference filtered flame archetypes

2.2.1. Optimization on Filtered Planar Flames (FPF)

The first solution to build-up the filtered optimized scheme is to isolate the impact of sub-grid scale wrinkling from the filtering process. The identification of diffusion and kinetic rate parameters is split in two steps.

i) A collection of 1-D freely propagating laminar flames is computed for various equivalence ratios ϕ using a detailed chemical scheme and then filtered in the spatial dimension with a Gaussian filter of size Δ. This collection of Filtered Planar Flames (FPF) provides the filtered reference thermo-chemical quantities $\widetilde{\varphi}_{\rm FPF} = \widetilde{\varphi}_{\rm FPF}(x, \phi, \Delta)$ on which is trained the optimized scheme. This step leads to the identification of parameters $\mathcal{A}^*_{\rm FPF} = (A^*_{j,\rm FPF}, E^*_{a,j,\rm FPF}, n^*_{ij,\rm FPF})$ and $\alpha^*_{\rm FPF}$, function of ϕ and Δ as shown in Tab. 1.

ii) The introduction of sub-grid scale flame wrinkling Ξ_Δ is done *a posteriori* by multiplying pre-exponential constants and the diffusive correction coefficient by Ξ_Δ: $\mathcal{A}^* = (\Xi_\Delta A^*_{j,\rm FPF}, E^*_{a,j,\rm FPF}, n^*_{ij,\rm FPF})$ and $\alpha^* = \Xi_\Delta \alpha^*_{\rm FPF}$.

This operation, which is common in many turbulent LES combustion model [12, 14] does not affect the filtered flame structure but ensures that the filtered flame propagates at a speed $S_\Delta = \Xi_\Delta S_l$, where S_l is the unstretched laminar flame speed. However, as pointed out in [20], this assumption includes biases in the prediction of some pollutants, such as CO. To address this issue, wrinkling patterns can be included in the filtering process.

2.2.2. Optimization on Filtered Wrinkled Flamelets (FWF)

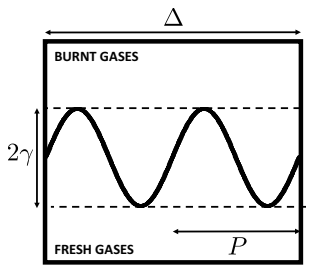

Figure 1: Schematical view of sub-filter sinusoidal flame pattern.

A 2-D wrinkled flame pattern, shown in Fig. 1, is manufactured by approximating the flame front position by a sinusoidal function of amplitude γ and wavelength P. Embedded in a 2-D square of size Δ, this flame pattern of wrinkling Ξ_Δ contains a number of wavelengths $n_\Delta = \Delta/P$. Assuming that the flame is in the flamelet regime, the 2-D flame structure is manufactured from a 1-D laminar premixed flame computed with detailed chemistry. The reconstruction algorithm as well as the possible physical range covered by wrinkling parameters γ and n_Δ are detailed in [20]. The manufactured wrinkled flame is then 2-D filtered and, due to the periodicity of the sine function, filtered thermo-chemical variables re-

duce to a single dimension x, perpendicular to the flame front propagation: $\widetilde{\varphi}_{\mathrm{FWF}} = \widetilde{\varphi}_{\mathrm{FWF}}(x, \phi, \Delta, n_\Delta, \Xi_\Delta)$. The filtered database serves as an ensemble of targets for the filtered optimized scheme. This step leads to the identification of parameters $\mathcal{A}^* = (\mathcal{A}^*_{j,\mathrm{FWF}}, E^*_{a,j,\mathrm{FWF}}, n^*_{ij,\mathrm{FWF}})$ and $\alpha^* = \alpha^*_{\mathrm{FWF}}$. The parameter dependencies of the new filtered optimized scheme are listed in Tab. 1. While the simplified approach to represent wrinkled flames neglects several physical phenomena, such as local variations in temperature due to turbulence, it has been shown to recover with reasonable accuracy the effect of sub-filter wrinkling on pollutants formation [20].

Table 1: Summary of Filtered Optimized Model with FPF and FWF flame libraries.

	FPF	**FWF**
$\boldsymbol{A^*_j}$	$\Xi_\Delta A^*_{j,\mathrm{FPF}}(\phi, \Delta)$	$A^*_{j,\mathrm{FWF}}(\phi, \Delta, \Xi_\Delta, n_\Delta)$
$\boldsymbol{E^*_{a,j}}$	$E^*_{a,j,\mathrm{FPF}}(\phi, \Delta)$	$E^*_{a,j,\mathrm{FWF}}(\phi, \Delta)$
$\boldsymbol{n^*_{ij}}$	$n^*_{ij,\mathrm{FPF}}(\phi, \Delta)$	$n^*_{ij,\mathrm{FWF}}(\phi, \Delta)$
$\boldsymbol{\alpha^*}$	$\Xi_\Delta \alpha^*_{\mathrm{FPF}}(\phi, \Delta)$	$\alpha^*_{\mathrm{FWF}}(\phi, \Delta, \Xi_\Delta, n_\Delta)$

2.2.3. Influence of FPF and FWF archetypes on the filtered chemical flame structure

FPF and FWF archetypes are both manufactured from a 1-D laminar premixed methane/air detailed chemistry solution obtained using the GRI3.0 mechanism [23] at an equivalence ratio $\phi = 0.75$. Filtered temperature and CO mass fractions are plotted in Fig. 2. FWF solutions (lines) are shown for one flame pattern ($n_\Delta = 1$) but for different values of sub-grid scale flame winkling. For $\Xi = 1$, the FWF profiles degenerate as expected towards the

FPF solution (symbols). When the sub-grid scale flame wrinkling increases, the filtered thermal layer is thickened. Fig. 2 (right) shows that the CO peak is also enhanced by the sub-grid scale wrinkling. The total mass of CO contained in the filter box of surface Δ^2 is: $\mathcal{M}^{\Delta}_{CO}(\Xi_\Delta) = \int_{\Delta^2} \rho Y_{\rm CO} {\rm d}s$.

The ratio $\mathcal{M}^{\Delta}_{CO}(\Xi_\Delta)/\mathcal{M}^{\Delta}_{CO}(\Xi_\Delta = 1)$ is plotted in terms of Ξ_Δ in Fig. 3 for two LES filter size values: $\Delta = 4\delta^0_l$ and $8\delta^0_l$, where δ^0_l is the laminar flame thickness. To avoid superposition of sine branches, the possible number of flame patterns within the filter box is limited to $n^{max}_\Delta = E[\Delta/2\delta^0_l]$, where $E[.]$ refers to the integer part of a number. The normalized mass of CO is therefore shown in Fig. 3 for all possible number of flame patterns ($n_\Delta = (1, 2)$ for $\Delta = 4\delta^0_l$ and $n_\Delta = (1, 2, 3, 4)$ for $\Delta = 8\delta^0_l$). A significant increase of CO mass is first observed when the SGS wrinkling grows. The mass of CO remains however lower than the value (dashed line) obtained under infinitely thin flame front assumption: $\mathcal{M}^{\Delta}_{CO}(\Xi_\Delta) = \Xi_\Delta \mathcal{M}^{\Delta}_{CO}(\Xi_\Delta = 1)$. This is an effect due to the non-zero Y_{CO} equilibrium value [20]. Moreover, n_Δ has little impact on the mass of CO.

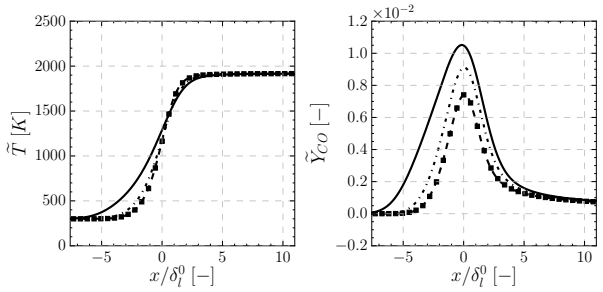

Figure 2: Illustration of the FPF and FWF flamelet libraries for $\phi = 0.75$, $\Delta = 4\delta^0_l$ and $n_\Delta = 1$. Legend: ■ ■ FPF flame. - - - FWF flamelet with $\Xi_\Delta = 1$. - . - FWF flamelet with $\Xi_\Delta = 1.5$. — FWF flamelet with $\Xi_\Delta = 2.4$.

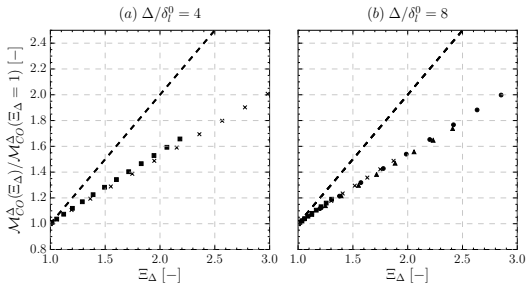

Figure 3: Normalized mass of CO in a subfilter box as a function of Ξ_Δ for $\phi = 0.75$ and two different filter sizes $4\delta_l^0$ and $8\delta_l^0$. Squares: $n_\Delta = 1$. Crosses: $n_\Delta = 2$. Triangles: $n_\Delta = 3$. Circles: $n_\Delta = 4$. Dashed line: unitary line $\mathcal{M}_{CO}^{\Delta}(\Xi_\Delta) = \Xi_\Delta \mathcal{M}_{CO}^{\Delta}(\Xi_\Delta = 1)$.

3. Filtered mechanism generation

In the present work, the COPLES method is applied to predict both the thermal flame structure, including heat release and flame propagation speed, and the CO production. The chemical scheme retained as a basis for the optimization procedure is based on the virtual chemistry concept [9, 10, 11]. This strategy relies on the optimization of a virtual mechanism composed of virtual reactions and virtual species whose properties are also optimized. The scheme is first made of the following two-step main virtual mechanism which converts CH_4 and O_2 into an intermediate species (I) which is then transformed through into a set of N_p virtual products P_k.

$$\alpha_{CH_4} CH_4 + \alpha_{O_2} O_2 \rightarrow \alpha_I I \tag{R1}$$

$$\alpha_I I \rightarrow \sum_{k=1}^{k=N_p} \alpha_{P_k} P_k \tag{R2}$$

The number of virtual products (here N_p=4) as well as the stoichiometric
174 coefficients α_{P_k} are optimized to retrieve real burnt gases temperature and enthalpy over the whole range of equivalence ratio conditions, as detailed in [11]. α_F, α_{Ox}, α_I are given by fuel composition.

177 Complementary independent virtual sub-mechanisms are devoted to the prediction of real pollutant species such as CO, NOx or soot precursors (PAH). By dedicating each sub-mechanism to a unique pollutant prediction,
180 this approach enables an efficient separation between slow and rapid chemical species. The following complementary virtual sub-mechanism is added here to predict the CO mass fraction:

$$\alpha_F F + \alpha_{Ox} Ox \rightarrow CO \tag{R3}$$

$$CO \rightleftharpoons V_1 \tag{R4}$$

183 where CO is the targeted pollutant species and V_1 is a virtual species. Free Gibbs energy of reaction (R4) is identified to retrieve the CO mass fraction at equilibrium conditions [11].

186 The COPLES method is then applied to optimize the molecular diffusion constant $\alpha^*$and the kinetics rate parameter $\mathcal{A}^*$ required to close Eq. 3. As the main virtual mechanism is independent from the virtual CO sub-mechanism,
189 the optimization process will be performed sequentially.

i) The diffusion constant α^*_{Main} and kinetics parameters $\mathcal{A}^*_{Main}$ of reactions (R1)-(R2) are first optimized to retrieve the temperature profile and the flame
192 propagation speed over a wide range of sub-grid scale wrinkling conditions. The objective function introduced in Eq. 5 is therefore defined with $\widetilde{\varphi} = \widetilde{T}(x)$

and $f_\varphi = S_\Delta$, where S_Δ is the filtered flame consumption speed. Reference database is made of the filtered flame archetypes presented in section 2.2.

ii) Parameters α^*_{CO} and $\mathcal{A}^*_{CO}$ relative to reactions (R3)-(R4) are then optimized to retrieve the CO production and consumption. The same reference database is used with a different objective function: $\widetilde{\varphi} = \widetilde{Y}_{CO}(x)$ and $f_\varphi = \mathrm{Max}(Y_{CO})$.

The optimized pre-exponential constant of (R3), written A^*_3, and the optimized parameter α^*_{CO} obtained when using FPF and FWF flames as optimization targets are illustrated in Fig. 4 for a filter size $\Delta = 4\delta^0_l$. Both pre-exponential constant and diffusion factor differ rapidly as the sub-grid scale flame wrinkling increases.

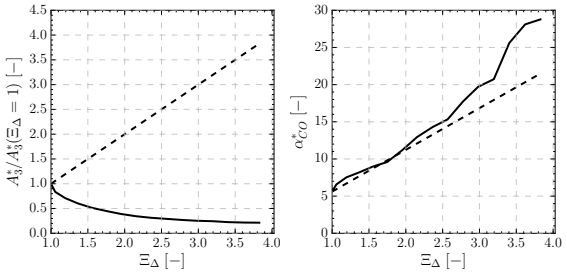

Figure 4: Evolution of A^*_3 and α^*_{CO} with the wrinkling factor for $\Delta = 4\delta^0_l$ and $n_\Delta = 2$. Legend: **- - -** COPLES-FPF model. — COPLES-FWF model.

4. Results

4.1. 1-D flame computations

To verify the realizability of COPLES modeling, filtered optimized schemes trained on FWF and FPF archetypes are used to compute 1-D planar fil-

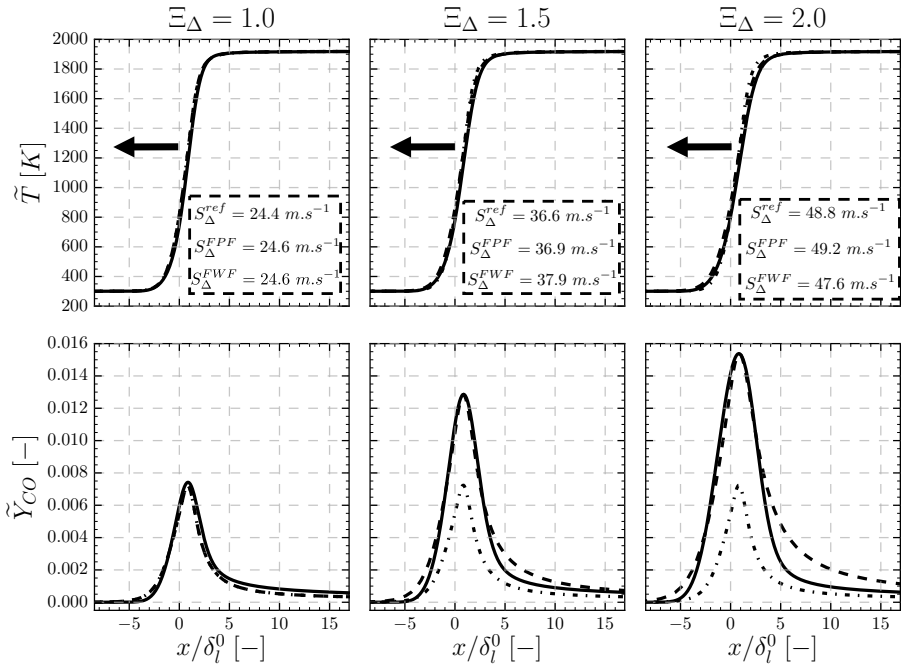

Figure 5: Evaluation of the performance of the COPLES modeling strategy on 1-D flames for an equivalence ratio $\phi = 0.75$. n_Δ is set to 2 and Δ to $4\delta_l^0$. Legend: — Reference flames. **- . -** COPLES-FPF model. **- - -** COPLES-FWF model.

tered premixed flames, wrinkled at the sub-grid scale, at an equivalence ratio $\phi = 0.75$ and with $n_\Delta = 2$. Figure 5 shows that COPLES solutions match as desired the FWF archetypes for different values of wrinkling factor. Note that the case $\Xi_\Delta = 1$ corresponds to a filtered laminar premixed flame. While the flame consumption speed added in Fig. 5 remains well predicted for all values of Ξ_Δ, the COPLES-FPF does not capture the influence of the sub-grid scale flame wrinkling on the filtered flame structure.

4.2. LES of a turbulent premixed burner: the Cambridge configuration.

The Cambridge SwB burner jointly studied at Cambridge University and Sandia laboratories [21] is selected to challenge the proposed LES combustion model. The burner is composed of a central bluff-body and two concentric annular tubes in which CH_4/air mixtures are flowing. In the retained operating conditions, a mixture with mean velocity $U_i = 8.31$ m/s and equivalence ratio $\phi_i = 0.75$ flows in the inner tube while a mixture of mean velocity $U_o = 18.7$ m/s and equivalence ratio $\phi_o = 0.75$ flows through the outer one. The burner is isolated by a large co-flow with mean velocity $U_{cf} = 0.4$ m/s. Details about the burner can be found in [21].

The YALES2 low-Mach number solver [24] is retained to solve the conservation equations. It features a fourth-order finite volume discretization and a fourth-order time integration using an explicit temporal scheme. An unstructured mesh containing 6 Million nodes and with a mesh size $\Delta_x = 0.5$ mm within the flame front is used. The flow field is transported using a standard low Mach formulation for the equations along with the Sigma model [25] for Reynolds sub-grid stresses.

The tested turbulent combustion models tested are the dynamic TFLES [14] and the COPLES models. The virtual chemical schemes described by reactions (R1)-(R2) and (R3)-(R4) are selected for chemistry modeling. COPLES schemes are optimized on either FPF or FWF archetypes, accordingly to section 2.2. A simple model has been derived for n_Δ in [20] by assuming infinitely thin flame front. Recent simulations of the Cambridge configuration performed using tabulated chemistry based on FWF archetypes however showed a small influence of n_Δ on the LES solutions [20]. n_Δ is hence

set constant to 2 in the simulations. The filter size retained to generate the reference database is $\Delta = 4\delta_l^0$, enabling a resolution of 5 nodes across the flame reaction zone. The corresponding TFLES thickening factor is approximately 5 throughout the flame front. The wrinkling factor is computed using the modified Charlette model [26]. In accordance with previous studies of the Cambridge burner [27], the fractal dimension is set to $\beta = 0.5$.

Instantaneous 2-D views of CO mass fraction predicted by both COPLES-FPF and COPLES-FWF simulations are qualitatively compared in Fig. 6 (left). The amount of CO mass fractions predicted by COPLES-FPF in the reactive layer remains identical for all axial positions. A similar quantity of CO produced is found in COPLES-FWF simulation in the vicinity of the bluff body. However, the amount of CO predicted by the COPLES-FWF simulation significantly increases in the downstream direction, from 2 cm above the burner exit. This enhancement of CO production is due to the sub-grid scale flame wrinkling, as shown in Fig. 6 (right).

To obtain statistics, filtered temperature and species mass fraction are averaged over 6 flow through times. Means of filtered functions can be compared to means of non-filtered experimental data when the mean flame brush is much higher than the filter size [28]. However, as the mean flame brush is here close to the LES filter size for $z < 30mm$, the mean experimental quantities cannot be directly compared to simulated means. The experimental profiles are then first filtered with the LES filter at the filter size $\Delta = 4\delta_l^0$. As thermo-chemical quantities gradients are dominated by radial contributions, filtering is done in 1-D on the radial axis. This approach is justified by the fact that experimental probes averaging volumes are much

smaller than Δ (temperature and major species measurements are limited by the sampling resolution of 103 μm and the laser beam diameters of 0.22 mm [21]) and the LES filtering hence predominates. The impact of filtering on both mean experimental profiles of temperature and CO mass fraction is significant as shown in Fig. 7 for axial position z=10mm.

Fig. 7 shows the mean temperature and the mean CO mass fractions at different axial positions z in the burner. Agreement on the mean temperature is fair for any of the turbulent combustion models, with only slight discrepancies on the flame opening angle. Pronounced differences between models are observed for mean $\widetilde{Y}_{CO}$. TFLES modeling significantly overestimates the CO mass fraction at all the axial positions. This overestimation of intermediate species profiles by the thickening operator is inherent to the TFLES approach, as discussed in [9, 20]. Filtered Optimized Chemistry improves significantly the peak of CO prediction. COPLES-FPF and COPLES-FWF give similar results below z=30 mm, where the flame wrinkling is moderate. However, for z=40 mm and z=50 mm, the introduction of wrinkling in filtered flame structure improves significantly predictions.

Predicted profiles are however thinner than experimental data. These discrepancies may be attributed to differential diffusion effects, significant in this configuration [29], but which are not captured in the present virtual mechanism formulation. Measurements show that differential diffusion implies an increase of the atomic equivalence ratio from 0.75 to 0.8 across the flame front[29]. As more CO is produced when $\phi = 0.8$, experimental profiles are expected to be higher than simulations, as observed in Fig. 7.

The following post-processing aims at removing the error induced by the

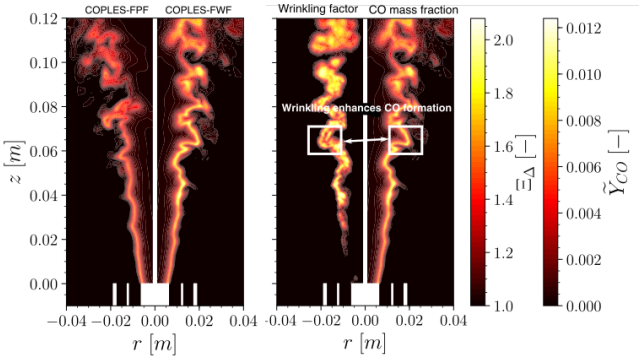

Figure 6: 2-D instantaneous fields on the plane $\theta \equiv 0\ [\pi]$. Left: comparison between $\widetilde{Y}_{CO}$ field obtained with COPLES-FPF (left) and COPLES-FWF (right) models. Right: comparison between Ξ_Δ (left) and $\widetilde{Y}_{CO}$ (right) from COPLES-FWF simulations.

omission of differential diffusion effects in the present simulations. The mass of CO per unit of axial length is computed for that purpose in cylindrical coordinates as follows:

$$\mathcal{I}_{CO}^{z=z_0} = \int_{\theta=0}^{2\pi} \left(\int_{r=0}^{R} r\{\widetilde{Y}_{CO}\}(r,\theta)\mathrm{d}r \right) \mathrm{d}\theta \tag{6}$$

where $\{.\}$ refers to Favre averaging in time and R is a radius covering the entire reaction zone up to the co-flow where $\widetilde{Y}_{CO}$ vanishes. Experiments show that the equivalence ratio variation along r induced by differential diffusion, remains roughly identical at any axial locations [29]. By selecting as a reference the plane located at $z = 10mm$, where the sub-grid scale flame wrinkling is resolved ($\Xi_\Delta \approx 1$), the relative mass of CO per unit of axial length is therefore defined as $\delta\mathcal{I}_{CO}^z = \mathcal{I}_{CO}^z - \mathcal{I}_{CO}^{z=10mm}$. $\delta\mathcal{I}_{CO}^z$ is plotted against z for experimental data and each of the simulations in Fig. 8. While TFLES over-estimates the CO integral evolution, the model featuring lami-

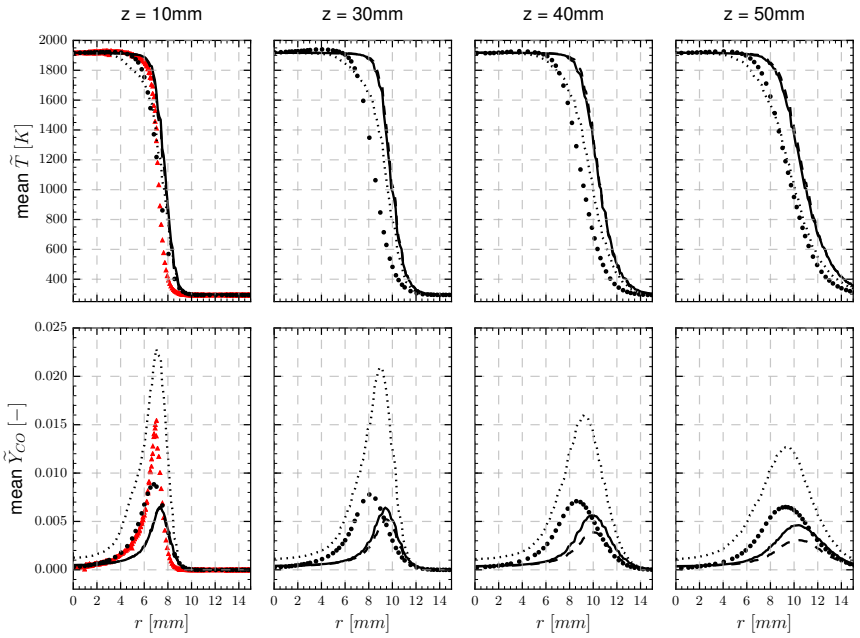

Figure 7: Radial profiles of mean $\widetilde{Y}_{CO}$. Black circles: filtered experimental data. Red triangles: non filtered experimental data (shown for z=10mm). Dotted lines: TFLES model. Dashed lines: COPLES-FPF. Plain lines: COPLES-FWF.

nar premixed flames as optimization targets under-estimates it because the influence of growing sub-grid scale flame wrinkling is not considered. Adding the wrinkling influence in the target flame archetype leads to an excellent agreement with experimental data.

5. Conclusion

A new methodology developed to model the influence of sub-grid scale wrinkling on flame structure initially developed in a tabulated chemistry context [20] has been extended to transported chemistry. Conservation equations are re-written with optimized Arrhenius coefficients and molecular diffusion

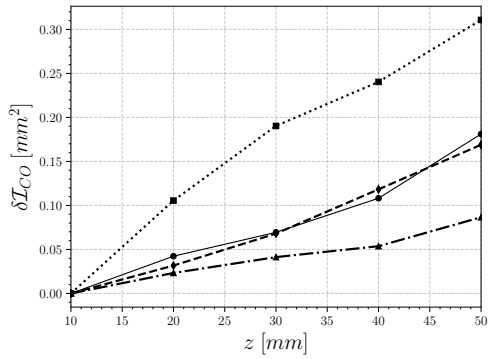

Figure 8: Integral of CO mass fractions $\mathcal{I}_{CO}$ in planes (r, θ) as a function of the axial positions z. Legend: ●—● Experimental data. ▲ - · - ▲ COPLES-FPF model. ♦- - -♦ COPLES-FWF model. ■ · · · ■ TFLES model.

factor to retrieve a set of reference flames. Two approaches have been studied. In a first case, the optimization is done by targeting laminar premixed flames and including wrinkling with the standard technique. A second possibility is to optimize coefficients on the newly developed 2-D manufactured wrinkled flames proposed in [20]. The simulation of a 3-D turbulent premixed burner has shown a significant advantage of the models based on optimization over a classical TFLES model which tends to over-estimate CO quantities. Moreover, adding the influence of wrinkling thanks to the FWF archetype improves significantly the results quality. Discrepancies observed between LES and experiments are attributed to the omission of preferential species transport in the model, which has a significant influence on the chemical structure of the turbulent flame configuration investigated here [29]. Future work will aim at improving the optimization of molecular diffusion in order to include these complex transport phenomena in the Filtered Optimized

Chemistry model.

Acknowledgments

This work was performed using HPC resources from GENCI-IDRIS (Grant 2017-A0012B00164).

References

[1] S. B. Pope, Small scales , many species and the manifold challenges of turbulent combustion, Proc. Combust. Inst. 34 (2013) 1–31.

[2] P. Pepiot-Desjardins, H. Pitsch, An efficient error-propagation-based reduction method for large chemical kinetic mechanisms, Combust. Flame 154 (2008) 67–81.

[3] B. Fiorina, D. Veynante, S. Candel, Modeling combustion chemistry in large eddy simulation of turbulent flames, Flow Turbul. Combust. 94 (2015) 3–42.

[4] J. A. V. Oijen, A. Donini, R. J. M. Bastiaans, J. H. M. T. Boonkkamp, L. P. H. D. Goey, State-of-the-art in premixed combustion modeling using flamelet generated manifolds, Prog. Energy Combust. Sci. 57 (2016) 30–74.

[5] B. Fiorina, O. Gicquel, L. Vervisch, S. Carpentier, N. Darabiha, Approximating the chemical structure of partially premixed and diffusion counterflow flames using fpi flamelet tabulation, Combust. Flame 140 (2005) 147–160.

[6] J. Lamouroux, M. Ihme, B. Fiorina, O. Gicquel, Tabulated chemistry approach for diluted combustion regimes with internal recirculation and heat losses, Combust. Flame 161 (2014) 2120–2136.

[7] T. Jaravel, E. Riber, B. Cuenot, G. Bulat, Large eddy simulation of an industrial gas turbine combustor using reduced chemistry with accurate pollutant prediction, Proc. Combust. Inst. 36 (2017) 3817–3825.

[8] A. Felden, L. Esclapez, E. Riber, B. Cuenot, H. Wang, Including real fuel chemistry in LES of turbulent spray combustion, Combust. Flame 193 (2018) 397–416.

[9] M. Cailler, N. Darabiha, D. Veynante, B. Fiorina, Building-up virtual optimized mechanism for flame modeling, Proc. Combust. Inst. (2017).

[10] G. Maio, M. Cailler, R. Mercier, B. Fiorina, Virtual chemistry for temperature and CO prediction in LES of non-adiabatic turbulent flames, Proc. Combust. Inst. 37 (2019) 2591–2599.

[11] M. Cailler, N. Darabiha, B. Fiorina, Development of a virtual optimized chemistry method. Application to hydrocarbon/air combustion, Combust. Flame 211 (2020) 281–302.

[12] T. Poinsot, D. Veynante, Theoretical and Numerical Combustion, 2005.

[13] B. Fiorina, R. Vicquelin, P. Auzillon, N. Darabiha, O. Gicquel, D. Veynante, A filtered tabulated chemistry model for LES of premixed combustion, Combust. Flame 157 (2010) 465–475.

[14] O. Colin, F. Ducros, D. Veynante, T. Poinsot, A thickened flame model for large eddy simulations of turbulent premixed combustion, Phys. Fluids 12 (2000) 1843–1863.

[15] F. Charlette, C. Meneveau, D. Veynante, A power-law flame wrinkling model for LES of premixed turbulent combustion Part I: non-dynamic formulation and initial tests, Combust. Flame 131 (2002) 159–180.

[16] D. C. Haworth, Progress in probability density function methods for turbulent reacting flows, Prog. Energy Combust. Sci. 36 (2010) 168–259.

[17] M. Cailler, R. Mercier, V. Moureau, D. Nasser, B. Fiorina, Prediction of co emissions in les of turbulent stratified combustion using virtual chemistry, 55th AIAA Aerospace Sciences Meeting, AIAA SciTech Forum (2017).

[18] A. Abou-Taouk, B. Farcy, P. Domingo, L. Vervisch, S. Sadasivuni, L.-E. Eriksson, Optimized Reduced Chemistry and Molecular Transport for Large Eddy Simulation of Partially Premixed Combustion in a Gas Turbine, Combust. Sci. Technol. 188 (2015) 21–39.

[19] V. Moureau, P. Domingo, L. Vervisch, From large-eddy simulation to direct numerical simulation of a lean premixed swirl flame: Filtered laminar flame-pdf modeling, Combust. Flame 158 (2011) 1340–1357.

[20] R. Mercier, C. Mehl, B. Fiorina, V. Moureau, Filtered Wrinkled Flamelets model for Large-Eddy Simulation of turbulent premixed combustion, Combust. Flame 205 (2019) 93–108.

[21] M. S. Sweeney, S. Hochgreb, M. J. Dunn, R. S. Barlow, The structure of turbulent stratified and premixed methane/air flames I: Non-swirling flows, Combust. Flame 159 (2012) 2896–2911.

[22] P. Nilsson, X. Bai, Effects of flame stretch and wrinkling on co formation in turbulent premixed combustion, Proc. Combust. Inst. 29 (2002) 1873–1879.

[23] G. Smith, D. M. Golden, M. Frenklach, N. W. Moriarty, B. Eiteneer, M. Goldenberg, C. T. Bowman, R. K. Hanson, S. Song, W. C. Gardiner, Jr, V. V. Lissianski, Z. Qin, GRI3.0. Available at *http* : *//www.me.berkeley.edu/gri_mech/*.

[24] V. Moureau, P. Domingo, L. Vervisch, Design of a massively parallel CFD code for complex geometries, Comptes Rendus Mécanique 339 (2011) 141–148.

[25] F. Nicoud, H. B. Toda, O. Cabrit, S. Bose, J. Lee, Using singular values to build a subgrid-scale model for large eddy simulations, Phys. Fluids 23 (2011).

[26] G. Wang, M. Boileau, D. Veynante, Implementation of a dynamic thickened flame model for large eddy simulations of turbulent premixed combustion, Combust. Flame 158 (2011) 2199–2213.

[27] R. Mercier, T. Schmitt, D. Veynante, B. Fiorina, The influence of combustion SGS sub models on the resolved flame propagation. Application to the LES of the Cambridge stratified flames, Proc. Combust. Inst. 35 (2015) 1259–1267.

[28] L. Vervisch, P. Domingo, G. Lodato, D. Veynante, Scalar energy fluctuations in Large-Eddy Simulation of turbulent flames: Statistical budgets and mesh quality criterion, Combust. Flame 157 (2010) 778–789.

[29] R. S. Barlow, M. J. Dunn, M. S. Sweeney, S. Hochgreb, Effects of preferential transport in turbulent bluff-body-stabilized lean premixed CH 4/air flames, Combust. Flame 159 (2012) 2563–2575.